Journal of Biomedical Optics

SPIEDigitalLibrary.org/jbo

Photoacoustic tomography through a whole adult human skull with a photon recycler

Liming Nie
Xin Cai
Konstantin Maslov
Alejandro Garcia-Uribe
Mark A. Anastasio
Lihong V. Wang

SPIE

Photoacoustic tomography through a whole adult human skull with a photon recycler

Liming Nie,* Xin Cai,* Konstantin Maslov, Alejandro Garcia-Uribe, Mark A. Anastasio, and Lihong V. Wang
Washington University, Department of Biomedical Engineering, St. Louis, Missouri 63130

Abstract. Photoacoustic tomography (PAT) of the human brain is challenging due to the fact that the skull strongly absorbs and scatters light, and attenuates and distorts ultrasound as well. For the first time, we demonstrated the feasibility of PAT through a whole adult human skull. A photon recycler (PR) was built to increase light transmittance through the skull. Both a graphite target and a canine brain were imaged through the skull. Use of the PR was found to improve the photoacoustic signal-to-noise ratio by a factor of 2.4. In addition, subtraction of photoacoustic signals that arise from light absorption within the skull significantly improved the contrast of the target. Our results indicate that PAT can potentially be applied to *in vivo* human brain imaging. [DOI: 10.1117/1.JBO.17.11.110506]

Keywords: human brain imaging; photoacoustic tomography; optical scattering; skull absorption; subtraction imaging; transcranial imaging.

Paper 12630L received Sep. 22, 2012; revised manuscript received Oct. 16, 2012; accepted for publication Oct. 17, 2012; published online Nov. 2, 2012.

1 Introduction

Technological advancements in brain imaging can facilitate the understanding of neural activities and cognitive phenomena. Magnetic resonance imaging (MRI) is the most widespread approach in the field of functional brain mapping.[1] However, MRI employs costly and nonportable imaging equipment and provides weak functional signals. Optical imaging is desirable because high functional hemoglobin contrast can be directly measured. However, pure optical imaging such as diffuse optical tomography (DOT) in the human brain suffers from its inherently low spatial resolution.[2] Ultrasonography is commonly used for pediatric brain imaging before the closure of fontanelles. However, ultrasound specificity is limited by the low acoustic impedance contrast of soft brain tissues.[3] Moreover, ultrasound signals propagate two-ways through the skull and suffer low backscattering and much distortion. Photoacoustic (PA) tomography (PAT), combining the advantages of pure optical imaging and pure ultrasonic imaging,[4,5] suggests a potential solution for human brain imaging. PA signals are produced omnidirectionally, and PAT only experiences a one-way ultrasound transmission through the skull. Subsequently, PA signals are generally stronger and less distorted than the echo data in ultrasound imaging.

Previously, PAT of the brain was successfully conducted through a monkey skull but never through a human skull.[6–8] Since the human skull is greatly thicker than a monkey skull, light and ultrasound will be strongly attenuated, deteriorating the image quality more severely. In this letter, we report the first demonstration of PAT through an intact adult human skull. Because the human skull scatters light strongly,[9] we designed and constructed a photon recycler (PR) to reflect back-scattered light back to the skull. Differential PAT images were acquired to improve the contrast by subtracting the images corresponding to the skull only. A graphite phantom and the cerebral cortex of a canine brain were successfully imaged through the skull in the differential images.

2 Materials and Methods

A cylinder (7.6 cm diameter × 5.5 cm height) made from plastic polyvinyl (Lida Plastic Industry Co., Ltd. China) was used as the substrate of the PR. A hole (2.54 cm diameter × 2 cm height) was co-axially drilled into the cylinder for laser transmission. A parabolic surface was carved into the other side of the cylinder with the top center aligned with the hole. Titanium white pigment (Dick Blick Art Materials, IL) mixed with epoxy was painted on the surface, and further smoothed to improve light reflectivity.

A schematic and a photograph of the PAT system with PR are shown in Fig. 1(a) and 1(b), respectively. The PR was positioned on top of human skull to recycle the light scattered off of the skull. The light beam propagates through the central hole of the PR, and then is expanded by passing through a plano-concave lens (12.7 mm aperture, 0.42 NA) and a bi-concave lens (12.7 mm aperture, 0.5 NA) to illuminate the skull. The illumination source is a laser operating at 1064 nm wavelength (Vibrant HE 315I, Opotek, Inc., CA). The laser pulse has a repetition rate of 10 Hz and a pulse width of 5 ns. The fluence of each laser pulse on the top skull surface was well below 40 mJ/cm^2, the safety standard set by the American National Standards Institute (ANSI).[10]

The intact human skull was purchased (Skull Unlimited International Inc. Oklahoma City, OK) and was donated by an 83-year-old Caucasian male. The natural skull was fixed with the aid of dermestid carrion beetles. The skull was subsequently cleaned by use of hydrogen peroxide and a degreaser. The length, width, and height of the fixed skull were 22 cm, 15 cm and 15 cm, respectively. We expanded the foramen magnum to place samples inside the skull. The thickness of the skull is inhomogeneous, ranging from ~7 mm (temporal area) to ~11 mm (frontal area). The light transmittance at 1064 nm through the top of the fixed human skull was measured to be ~2.1%, which is similar to the computed light transmittance of a fresh skull reported in Refs. 9 and 11. Also the effects of fixation on the acoustic properties of skull have been demonstrated to be minor.[12] Because of this, fixed skulls have long been used for transcranial ultrasound research.[13] Therefore, a fixed skull can be employed as a study model for transcranial PAT.[9,12]

*These authors contributed equally to this work.

Address all correspondence to: Lihong V. Wang, Washington University, Department of Biomedical Engineering, St. Louis, One Brookings Drive, Saint Louis, Missouri 63110. Tel: 314-9356152; Fax: 314-9357448; E-mail: lhwang@biomed.wustl.edu

0091-3286/2012/$25.00 © 2012 SPIE

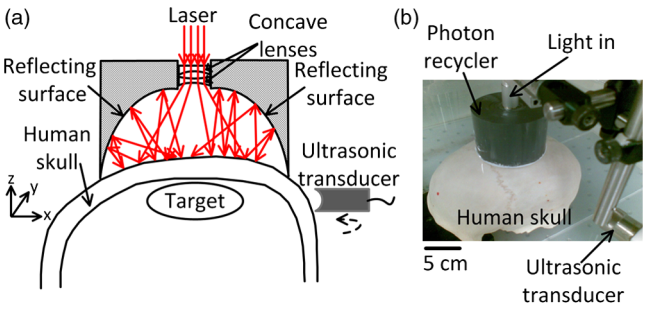

Fig. 1 (a) Schematic of the photon recycler (PR) reflecting backscattered photons back to the human skull for photoacoustic tomography (PAT). (b) Photograph of the PAT setup with PR.

3 Results and Discussion

A 1-MHz spherically focused transducer with a bandwidth of 70% (V314, Panametrics, Olympus) circularly scanned the skull to receive PA signals at 200 positions. The spatial resolution of our PAT system at the imaging center was estimated[7] to be ~1 mm, which is inversely proportional to the bandwidth of the transducer. The received PA signals were amplified by a 50-dB amplifier (5072 PR, Panametrics, Waltham, MA), then directed to a data-acquisition (DAQ) card (CS 14200; Gage Applied, Lockport, IL). The DAQ card was simultaneously triggered by the Q-switch signal from the laser to record the PA data in computer for back-projection reconstruction.[6,7] To compensate the PA amplitude for laser fluence fluctuation, the laser pulses were sampled by a photodiode (SM05PD1A, Thorlabs).

A triangular target composed of three graphite bars with a diameter of 0.7 mm was embedded in agar as the test phantom. Initially, the phantom was placed inside the empty skull but out of the light illumination area to acquire a baseline PAT image, shown in Fig. 2(a) (skull only). Then the phantom was moved to the cortical area under the light illumination without changing other experimental conditions to acquire a second PAT image, shown in Fig. 2(b). The PA signals in Fig. 2(b) are greater than signals in Fig. 2(a) due to the absorption contribution of the graphite. The triangular shape can be found in Fig. 2(b) despite the strong background signals from the skull. The differential image in Fig. 2(c) [Fig. 2(b) subtracted by Fig. 2(a)] reveals the triangle more clearly with a high signal to background contrast than that in Fig. 2(b). Each image was acquired five times to calculate the signal-to-noise ratio (SNR, defined as an amplitude ratio here), and the average images are shown. The standard deviation image of the five differential images is shown in Fig. 2(d). The difference between the PAT images acquired without PR (left column marked with 'Without PR') and with PR (right column marked with 'With PR') is that the latter have stronger signals than the former while the noise in standard derivation did not change significantly. That is because diffusely reflected light from the skull was recycled back toward the skull by the PR to generate more PA signals. Based on the respective five differential images acquired with and without PR, the SNR was found to be enhanced by the PR 2.4 times from 6.3 to 15.

After craniotomy on a 3-month-old canine, the brain was obtained and immediately immersed in 10% formalin solution to maintain the vasculature. All procedures in the animal experiments followed the protocols approved by the Institutional Animal Care and Use Committee at Washington University in St. Louis. PAT imaging of the canine brain cortex through the human skull with the PR was conducted with the same

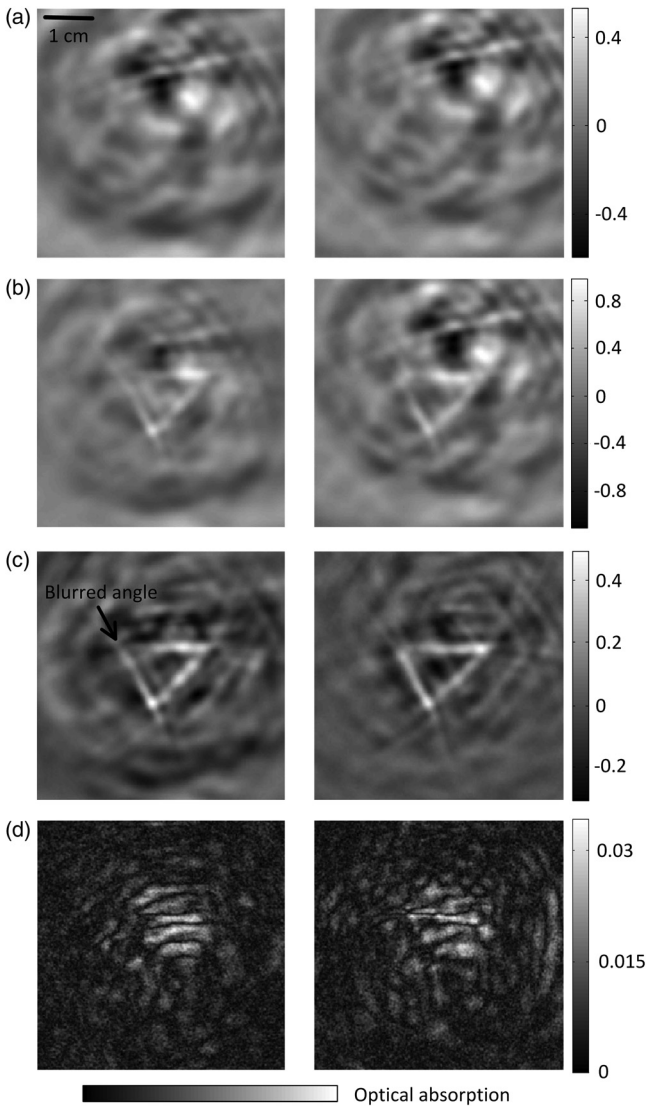

Fig. 2 PAT of a triangular target through the top area of a whole adult human skull. Each image was acquired five times to calculate the signal-to-noise ratio (SNR), and the average images are shown. (a) PAT images of the human skull only. (b) PAT images of the graphite triangle acquired through the human skull. (c) Differential images of (b) and (a). (d) Standard deviation maps of the five differential images. No PR was used for the panels in the left column marked with 'Without PR,' PR is used for the panels in the right column marked with 'With PR'.

procedure as employed in the aforementioned phantom experiment. The PAT image with only the skull present is shown in Fig. 3(a). After the canine brain cortex was positioned in the cortical area of the skull, a similarly distorted PAT image was obtained as displayed in Fig. 3(b). However, the differential PAT image shown in Fig. 3(c) [Fig. 3(a) subtracted from Fig. 3(b)] reveals brain features that are readily identifiable. Since high-frequency signals were more attenuated by the thick skull [shown as a top-view photograph in Fig. 3(e)], the surviving PA signals are low-pass filtered. As a result, the reconstructed images possess a slowly varying background and a lack of sharp features as shown in Fig. 3(c). After applying a high-pass filter with a cutoff frequency of ~100 KHz on the image in Fig. 3(c), many more features are clearly revealed as shown in Fig. 3(d). The background was suppressed at the expense of reducing the peak signal amplitude ~1.8 times. Eight main blood vessels

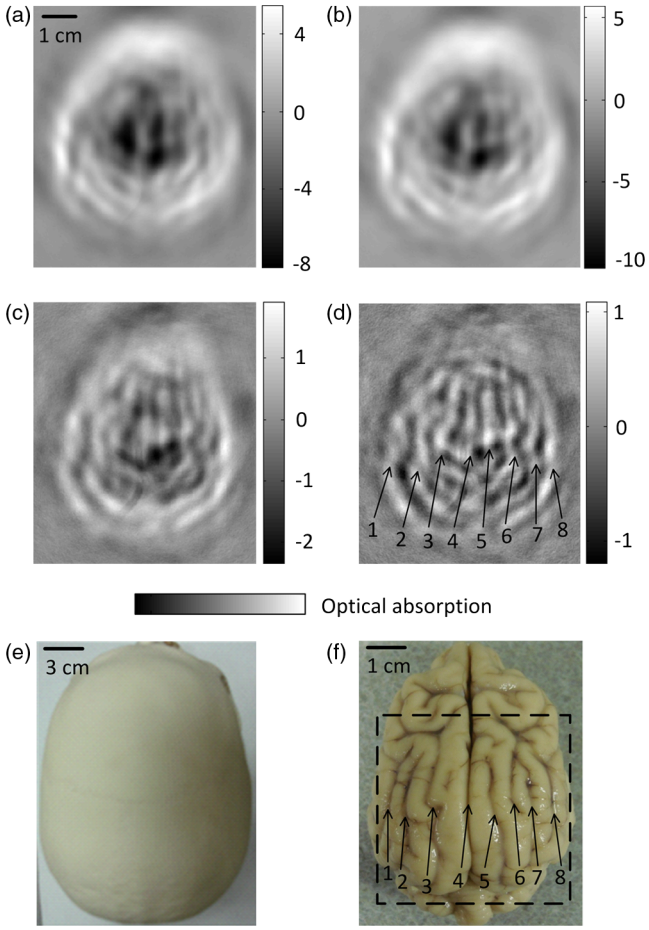

Fig. 3 PAT of a canine brain through the top area of the whole adult human skull with PR. (a) PAT image of the human skull only. (b) PAT image of a canine brain acquired through the human skull. (c) Differential image of (b) and (a). (d) Image from (c) after high-pass filtering. (e) Photograph of the human skull from a top view. (f) Photograph of the canine brain cortex.

were marked by numbered arrows, which have good correlation with the features in the photograph of the canine brain in Fig. 3(f).

Our experimental results demonstrate that light can penetrate the thick human skull and the produced PA signals are sufficiently detectable. A PR can effectively increase light transmittance through the human skull, thus enhance the imaging SNR. Subtraction imaging is a common method for analyzing changes in pairs of images such as functional MRI and computed tomography (CT) in a wide range of circumstances.[14,15] We can acquire differential PAT images of the human brain by imaging at consecutive time points, and/or before and after neural stimulation or injection of contrast agents. Therefore we can trace, monitor the dynamic change in regions of interest within the human brain. The targets in the PAT images were distorted and dislocated because of the mismatch of speed of sound between water and skull. Image quality can further be improved by use of advanced reconstruction algorithms that account for the presence of the skull, such as time-reversal methods.[8,16]

4 Conclusion

We believe that our results will accelerate the application of PAT to human brain imaging. PAT based on an ultrasonic transducer array or multiple transducers will accelerate data acquisition and permit real-time imaging. Moreover, multiwavelength PAT can be employed to compute oxygen saturation of hemoglobin, observing functional activities of the human cerebral cortex. Therefore, PAT can potentially be used for monitoring the blood-related pathological and physiological status of human brains.

Acknowledgments

We thank Ms. Sandra Matteucci for the close manuscript proofreading. We acknowledge support by the NIH awards R01 EB010049, R01 CA134539, R01 EB000712, U54 CA136398, and R01 EB008085. L. V. W. has a financial interest in Microphotoacoustics, Inc. and Endra, Inc., which, however, did not support this work.

References

1. B. B. Biswal et al., "Toward discovery science of human brain function," *Proc. Natl. Acad. Sci.* **107**(10), 4734–4739 (2010).
2. D. A. Boas, A. M. Dale, and M. A. Franceschini, "Diffuse optical imaging of brain activation: approaches to optimizing image sensitivity, resolution and accuracy," *Neuroimage* **23**(suppl 1), S275–S288 (2004).
3. S. W. Smith et al., "Feasibility study: real-time 3-D ultrasound imaging of the brain," *Ultrasound Med. Biol.* **30**(10), 1365–1371 (2004).
4. L. V. Wang and S. Hu, "Photoacoustic tomography: *in vivo* imaging from organelles to organs," *Science* **335**(6075), 1458–1462 (2012).
5. L. Nie, D. Xing, and S. Yang, "*In vivo* detection and imaging of low-density foreign body with microwave-induced thermoacoustic tomography," *Med. Phys.* **36**(8), 3429–3437 (2009).
6. X. Yang and L. V. Wang, "Monkey brain cortex imaging by photoacoustic tomography," *J. Biomed. Opt.* **13**(4), 044009 (2008).
7. L. Nie, Z. Guo, and L. V. Wang, "Photoacoustic tomography of monkey brain using virtual point ultrasonic transducers," *J. Biomed. Opt.* **16**(7), 076005 (2011).
8. C. Huang et al., "Aberration correction for transcranial photoacoustic tomography of primates employing adjunct image data," *J. Biomed. Opt.* **17**(6), 066016 (2012).
9. A. N. Bashkatov et al., "Optical properties of human cranial bone in the spectral range from 800 to 2000 nm," *Proc. SPIE* **6163**, 616310 (2006).
10. ANSI Laser Institute of America, "American national standard for safe use of lasers," ANSI Z136.1–2000, American National Standards Institute, New York (2000).
11. Y. Hoshi et al., "Reevaluation of near-infrared light propagation in the adult human head: Implications for functional near-infrared spectroscopy," *J. Biomed. Opt.* **10**(6), 064032 (2005).
12. F. Fry and J. Barger, "Acoustical properties of the human skull," *J. Acoust. Soc. Am.* **63**(5), 1576–1590 (1978).
13. J. Aubry et al., "Experimental demonstration of noninvasive transskull adaptive focusing based on prior computed tomography scans," *J. Acoust. Soc. Am.* **113**(1), 84–93 (2003).
14. M. Lell et al., "Clinical evaluation of bone-subtraction CT angiography (BSCTA) in head and neck imaging," *Eur. Radiol.* **16**(4), 889–897 (2006).
15. K. K. Kwong et al., "Dynamic magnetic resonance imaging of human brain activity during primary sensory stimulation," *Proc. Natl. Acad. Sci. U.S.A.* **89**(12), 5675–5679 (1992).
16. C. Huang et al., "Photoacoustic computed tomography correcting for heterogeneity and attenuation," *J. Biomed. Opt.* **17**(6), 061211 (2012).